



## ORIGINAL ARTICLE

# Atheroprotective remodelling of vascular dermatan sulphate proteoglycans in response to hypercholesterolaemia in a rat model

Roxana Oberkersch\*, Francesca Maccari<sup>†</sup>, Alicia I. Bravo<sup>‡</sup>, Nicola Volpi<sup>†</sup>, Silvina Gazzaniga<sup>§</sup> and Graciela C. Calabrese\*

\**Cátedra de Biología Celular y Molecular, Departamento de Ciencias Biológicas, Facultad de Farmacia y Bioquímica, Universidad de Buenos Aires, Junín, Ciudad Autónoma de Buenos Aires, Argentina*, <sup>†</sup>*Department of Life Science, University of Modena and Reggio Emilia, Modena, Italy*, <sup>‡</sup>*Hospital Eva Perón, San Martín, Buenos Aires, Argentina* and <sup>§</sup>*Departamento de Química Biológica, Facultad de Ciencias Exactas y Naturales, Universidad de Buenos Aires, Ciudad Universitaria, Pabellón, Ciudad Autónoma de Buenos Aires, Argentina*

## INTERNATIONAL JOURNAL OF EXPERIMENTAL PATHOLOGY

doi: 10.1111/iep.12072

Received for publication: 25 October 2013

Accepted for publication: 14 January 2014

### Correspondence

Graciela C. Calabrese  
Cátedra de Biología Celular y  
Molecular  
Departamento de Ciencias Biológicas  
Facultad de Farmacia y Bioquímica  
Universidad de Buenos Aires  
Junín 954, (C1113AAD) Ciudad  
Autónoma de Buenos Aires  
Argentina  
Tel.: 54-011-4964-8238  
Fax: 54-011-508-3645  
E-mail: gcalabe@ffybu.uba.ar

## SUMMARY

Proteoglycan accumulation within the arterial intima has been implicated in atherosclerosis progression in humans. Nevertheless, hypercholesterolaemia is unable to induce intimal thickening and atheroma plaque development in rats. The study was performed to analyse proteoglycans modifications in rats fed with a high-cholesterol diet to understand whether vascular wall remodelling protects against lesions. Sections obtained from rat aortas showed normal features, in intimal-to-media ratio and lipid accumulation. However, focal endothelial hyperplasia and neo-intima rearrangement were observed in high-cholesterol animals. Besides, hypercholesterolaemia induced an inflammatory microenvironment. We determined the expression of different proteoglycans from aortic cells by Western blot and observed a diminished production of decorin and biglycan in high-cholesterol animals compared with control ( $P < 0.01$  and  $P < 0.05$ , respectively). Versican was increased in high-cholesterol animals ( $P < 0.05$ ), whereas perlecan production showed no differences. No modification of the total content of glycosaminoglycans (GAGs) was found between the two experimental groups. In contrast, the chondroitin sulphate/dermatan sulphate ratio was increased in the high-cholesterol group as compared to the control (0.56 and 0.34, respectively). Structural alterations in the disaccharide composition of galactosaminoglycans were also detected by HPLC, as the ratio of 6-sulphate to 4-sulphate disaccharides was increased in high-cholesterol animals ( $P < 0.05$ ). Our results suggest that attenuation of decorin and biglycan expression might be an effective strategy to inhibit the first step in atherogenesis, although specific GAG structural modification associated with the development of vascular disease took place. Results emphasize the potential application of therapies based on vascular matrix remodelling to treat atherosclerosis.

### Keywords

aortic cells, atherosclerosis, dermatan sulphate proteoglycans, extracellular matrix

Factors that determine early atherosclerotic lesions are unknown, but the vascular extracellular matrix (ECM) appears to be involved. Two hypotheses, which directly or indirectly reflect ECM involvement, have been proposed to explain the early molecular events of this pathology. The first hypothesis is the response-to-retention hypothesis, which emphasizes that the interaction between ECM mole-

cules, particularly proteoglycans (PGs) and lipoproteins, is the key event in early atherogenesis (Williams & Tabas 1995; Camejo *et al.* 1998; Skalen *et al.* 2002). The second hypothesis is the chronic inflammation hypothesis (Ross 1999; Tedgui & Mallat 2006), in which the binding of cytokines and growth factors to ECM PGs may increase the residence time of these molecules in the extracellular

environment and modulate their functional activity dynamically (Camejo *et al.* 1995; Young & Murphy-Ullrich 2004; Groeneveld *et al.* 2005). Consequently, the expression and distribution of arterial PGs are significantly modulated during atherosclerosis and ageing (Tovar *et al.* 1998). For instance, human atherosclerosis-prone arteries express PGs, such as biglycan and decorin, in the outer layer of the intima of prelesional areas preceding lipid deposition (Nakashima *et al.* 2007). Besides, GAG chains attached to the protein core of PGs undergo specific structural modifications during the development of the disease. Elongated GAG chains have been reported in human early atherosclerotic lesions (Theocharis *et al.* 2002; Little *et al.* 2007). For instance, hyperelongated chondroitin sulphate (CS) chains of biglycan may be the key factor for atherosclerosis, because they enhance the low-density lipoprotein (LDL) binding affinity (Anggraeni *et al.* 2011).

As it is known, hypercholesterolaemia is a dominant risk factor for atherosclerosis. Cholesterol feeding has been used to increase serum cholesterol levels and then to assess hypercholesterolaemia-related metabolic disturbances in different animal models (Deepa & Varalakshmi 2005; Hachani *et al.* 2011; Raman *et al.* 2011). In contrast to that observed in humans, in rats, hypercholesterolaemia alone is unable to induce intimal thickening and atheroma plaque development, mainly as a consequence of the lack of cholesteryl ester transfer protein (CETP) (Hogarth *et al.* 2003; Hachani *et al.* 2010).

The aim of this study was to analyse quantitative and structural modifications of PGs in aortas isolated from rats upon treatment with a high-cholesterol diet, to understand whether vascular wall remodelling may protect against the atheroma lesions.

## Material and methods

### *Media and reagents*

Dulbecco's modified Eagle medium (DMEM), cholesterol and collagenase type IV, chondroitinase ABC, chondroitinase B and antibody against  $\beta$ -actin (A 2228) were purchased from Sigma Chem. (St. Louis, MO, USA). Foetal bovine serum (FBS) was from Natocor (Córdoba, Argentina). Antibodies included rabbit polyclonal antibody against decorin (H-80; sc-22753), goat polyclonal antibody against perlecan (L-20; sc-27449), rabbit polyclonal antibody against versican (H-56, sc-25831) and goat polyclonal antibody against biglycan (L-15, sc-27936) from Santa Cruz Biotechnology, Inc. (Dallas, TX, USA); biotinylated anti-rabbit IgG (H+L) (P0512) from Vector Laboratories Inc. (Burlingame, CA, USA) and anti-actin, clone 4 (Mab1501R) from Millipore (Temecula, CA, USA).

### *Animals and tissues*

This study was carried out on male Wistar rats weighing 180–200 g. Veterinary care was provided by the breeding

laboratories of the Faculty of Pharmacy and Biochemistry (University of Buenos Aires, Argentina).

### *Ethical approval*

The procedures used in this study are in accordance with the guidelines of the Committee on the use and care of animals of the Faculty of Pharmacy and Biochemistry, University of Buenos Aires (Argentina) in agreement with the Institutional Use Review Board of the University of Buenos Aires, which conforms with the Guide for the Care and Laboratory Animals published by the US National Institutes of Health (NIH Publication No. 85–23, revised 1996).

### *Experimental Protocol*

Animals ( $n = 18/\text{group}$ ) were housed in a controlled environment (22–24 °C and 12 h light/dark cycle from 8 a.m. to 8 p.m.) with food and water *ad libitum*. Rats were divided into two groups and fed with different dietary formulations for 30 days: the control group (C), fed with standard rat chow and drinking water, and the high-cholesterol group (H-Chol), fed with standard rat chow supplemented with 2% cholesterol and 1% cholic acid to favour emulsification of fats (Zulet *et al.* 1999).

At the end of the experimental period, all animals were fasted for 6 h and weighed. Blood obtained via cardiac puncture under anaesthesia was centrifuged at 1200 g, and total cholesterol (mM), high-density lipoproteins (HDL) (mM) and triglycerides (mM) were measured enzymatically in the supernatant (Wiener Laboratorios, Rosario, Argentina). The non-HDL cholesterol level was defined as the difference value between total cholesterol and HDL total cholesterol, involving the different fractions of lipoproteins: low-density lipoproteins, intermediate-density lipoproteins and very low density lipoproteins, including highly atherogenic lipoproteins as very low density lipoprotein remnants.

Rats were killed with an overdose of pentobarbital and aortas rapidly removed. Aorta segments were perfused with 1 ml of phosphate-buffered saline (PBS) containing 1000 U/ml of heparin. Once aortas were dissected out from the aortic arch, the adventitial layer was removed and the intimal and medial layers preserved in DMEM 20% FBS and immediately used. Alternatively, portions of aortic tissue were fixed in 10% formalin for histological studies.

### *Histological analyses*

Serial sections from aortas (8–10  $\mu\text{m}$ ) ( $n = 6$  per group) were stained with haematoxylin–eosin and Masson's Trichrome. Images were taken with a DP70 digital camera coupled to an Olympus BX40 microscope. Measures of intima and media thickness in different points around aorta's circumference were measured. This process was repeated on each of the histological sections ( $n = 30$  per group). Nuclear counting was performed on 30 histological sections per group.

Fragments from aortas were frozen in liquid nitrogen and stored at  $-80^{\circ}\text{C}$  until immunostaining with anti-decorin, anti-biglycan, anti-perlecan or anti-versican antibodies. Briefly, cryostat sections ( $5\text{--}8\ \mu\text{m}$ ) were fixed in acetone for 10 min at room temperature and incubated with normal horse serum to prevent non-specific binding by secondary antibodies, followed by an overnight incubation with optimal dilutions of each primary antibody (1:100). The ABC system was revealed with DAB (DAB Substrate Kit for peroxidase; Vector Laboratories).

#### RNA isolation and RT-PCR analysis

About 30 mg of aortic tissue was lysed and homogenized in 175  $\mu\text{l}$  of the RNA lysis buffer from the SV total RNA isolation system (Promega, Madison, WI, USA) to improve RNA extraction. Total RNA was extracted and purified according to the manufacturer's instructions and converted into the first-strand cDNA using oligo (dT) primers (Biodynamics, Argentina), recombinant RNAs in ribonuclease inhibitor (Promega) and M-MLV reverse transcriptase (Promega). For reverse transcriptase polymerase chain reaction (RT-PCR), 1  $\mu\text{l}$  of cDNA was used as starting volume to amplify the DNA; 0.3  $\mu\text{l}$  of recombinant Taq DNA polymerase (Invitrogen, Vila Guarani, Sao Paulo, Brazil), 1  $\mu\text{l}$  of the primer mix and 1.6  $\mu\text{l}$  of dNTPs (U1330, Promega) were mixed. Amplification was performed on the DNA thermal cycler 480 (Perkin-Elmer, Waltham, MA, USA) as follows: an initial denaturation step of 5 min at  $95^{\circ}\text{C}$ , and 35 cycles of 1 min at  $95^{\circ}\text{C}$ , and 1 min at  $55^{\circ}\text{C}$  for TNF- $\alpha$ .

#### $\beta$ -Actin was used as housekeeping gene

Primer pairs for TNF- $\alpha$  sense and anti-sense were synthesized by Alpha DNA (Montreal, Quebec, Canada), according to reported sequences (Feferman *et al.* 2005). Amplified DNA fragments for TNF- $\alpha$  and  $\beta$ -actin were resolved by electrophoresis in 1.5% ethidium bromide-agarose gels and scanned using Ultra Lum Electronic Dual Light <sup>TM</sup> Transilluminator (American Laboratory Trading Inc., Boston, MA, USA) a Kodak DC120 camera digital and Photoenhancer program, Kodak SAIC (Buenos Aires, Argentina). PCR products for TNF- $\alpha$  were expressed relative to  $\beta$ -actin.

#### Isolation of aortic cells

Aortic endothelial cells (ECs) and smooth muscle cells (SMCs) were isolated as previously described (Kobayashi *et al.* 2005). Briefly, ECs and SMCs were isolated after collagenase type IV treatment for 45 min at  $37^{\circ}\text{C}$  and collected by centrifugation at 200 g for 5 min. The pellet was immediately re-suspended in 20% FBS-DMEM. Viability of cell suspensions (approximately 95%) was evaluated by Trypan blue exclusion.

#### Western blot of isolated aortic cells

Isolated aortic cells were homogenized and fractionated by ultracentrifugation as described previously (Calabrese *et al.* 2009) to obtain the microsome. Glucose-6-phosphatase activity was determined as microsomal marker (Barfell *et al.* 2011).

Protein content was measured with the BCA kit (Pierce, Rockford, IL, USA). About 30  $\mu\text{g}$  of proteins taken from the C and H-Chol groups was loaded simultaneously onto 10% (wt/vol) (decorin and biglycan) or 6% (wt/vol) (versican and perlecan) sodium dodecyl sulphate-polyacrylamide gel electrophoresis (SDS-PAGE). After electrophoresis, proteins were transferred to nitrocellulose membranes. Membranes were incubated with one of the following primary antibodies: decorin (1:200), biglycan (1:200), versican (1:200) and perlecan (1:200) and revealed by incubation with the corresponding biotinylated antibody (biotinylated against: rabbit IgG or goat IgG; both from Vector Laboratories, Inc.), followed by incubation with the biotin avidin-peroxidase complex (Vectastain ABC Kit; Vector Laboratories, Inc.) and then revealed with DAB (DAB Substrate Kit for peroxidase; Vector Laboratories, Inc.). Developed bands were scanned and proteins were quantified by densitometry analysis using the Gel-Pro 3.1 program. Finally, the amount of each protein was normalized to the amount of actin that was revealed by mouse monoclonal anti-actin (Millipore) using the same immunoblotting method described above. Comparisons were made (in triplicate) between 3 animals from each group. Prestained molecular markers (Bio-Rad Laboratories, Hercules, CA, USA) were used to assess molecular weight. Coomassie blue staining was used to check the separation and transfer of the appropriate protein.

#### Isolation of total aortic GAGs

Aortas were cut into small pieces and processed to isolate GAGs as described previously (Leta *et al.* 2002). Briefly, the chloroform/methanol-treated aortas were rehydrated in 0.1 M sodium acetate buffer at  $4^{\circ}\text{C}$  (pH = 5), containing 5 mM cysteine and 5 mM EDTA for 24 h. Thereafter, total GAGs were isolated by proteolysis with papain, followed by subsequent cetylpyridinium and ethanol precipitations. Total GAGs content was estimated by determination of hexuronic acid concentration (Calabrese *et al.* 2004).

#### Characterization of aortic GAGs

Glycosaminoglycans were separated by agarose gel electrophoresis as previously reported (Volpi & Maccari 2006). Briefly, agarose gel was prepared at a concentration of 0.5% in 0.04 M barium acetate buffer pH 5.8. Plates with a thickness of 4–5 mm were prepared. Samples of 10  $\mu\text{l}$  dissolved in distilled water were layered. The electrophoretic run was performed in 0.05 M HCl for 180 min at 200 mA and in 0.04 barium acetate (buffered at pH 5.8 with acetic acid) for 60 min at 100 mA. After migration, the plate was

soaked in a solution of 0.2% cetylpyridinium chloride. After drying, the plate was stained with freshly prepared toluidine blue (0.2% in ethanol/water/acetic acid 50:49:1) for 30 min and destained with ethanol/water/acetic (50:49:1). Quantitative analysis of GAGs was performed with a densitometer composed of a Macintosh IIsi computer interfaced with Microtek Color Scanner from Microtek International Inc., Hsinchu, Taiwan. Aliquots of the extracts obtained were treated with chondroitinase ABC or chondroitinase B to produce CS and dermatan sulphate (DS) unsaturated disaccharides for structural characterization. Ten microlitres of each sample (10 mg/ml) was treated with 5 mU of each enzyme in 50  $\mu$ l of 100 mM Tris/150 mM sodium acetate buffer pH 8.0 at 37 °C for 12 h. The reaction was stopped by boiling the solutions for 1 min. The unsaturated disaccharides generated after enzymatic treatment were analysed by strong anion-exchange (SAX)-HPLC separation and detection at 232 nm. Isocratic separation was performed from 0 to 5 min with 0.05 M NaCl, pH 4.0, and linear gradient separation was performed from 5 to 9 min with 100% 0.05 M NaCl, pH 4.0 to 100% 1.2 M NaCl, pH 4.0. Flow rate was 1.2 ml/min. Disaccharides were quantified by reverse phase HPLC equipped with a fluorescence detector according to Volpi (Volpi 2010).

#### Statistical analysis

Data are expressed as mean  $\pm$  SD. Graph Pad Prism 4 (Graph Pad Software Inc., La Jolla, CA, USA) was used for statistical evaluation. The statistical analysis was performed with ANOVA followed by Bonferroni's test or Mann Whitney's test. Values of  $P < 0.05$  were considered significantly different from controls.

## Results

#### Plasma cholesterol levels

Hypercholesterolaemia was checked by dosage of serum total cholesterol after feeding animals for 30 days with a 2% cholesterol diet. Plasma cholesterol level was nearly twofold higher than that of those fed a normal diet ( $P < 0.05$ , H-Chol *vs.* C group; Table 1). Plasma triglycerides and high-density lipoprotein cholesterol (HDL) showed no differences between the two groups, whereas non-HDL cholesterol was increased in the H-Chol group compared with the control one (H-Chol *vs.* C group,  $P < 0.05$ ; Table 1).

**Table 1** Lipids levels in plasma. Results are means  $\pm$  SD ( $n = 18$ /group). Total cholesterol, triglycerides, HDL cholesterol and non-HDL cholesterol are mean values at the time of sacrifice; Mann Whitney's test

Treatment groups	Total cholesterol (mM)	Triglycerides (mM)	HDL cholesterol (mM)	Non-HDL cholesterol (mM)
Control	1.97 $\pm$ 0.23	1.37 $\pm$ 0.45	1.41 $\pm$ 0.21	0.63 $\pm$ 0.10
High-Cholesterol	3.63 $\pm$ 0.61*	1.04 $\pm$ 0.50	1.59 $\pm$ 0.25	2.01 $\pm$ 0.47 <sup>#</sup>

\* $P < 0.05$ , H-Chol *vs.* control group; <sup>#</sup> $P < 0.05$ , H-Chol *vs.* control group.

Similarly, body weight and blood pressure were not affected by dietary hypercholesterolaemia (data not shown).

#### Histological analysis

Aortas from the control group presented flattened and inconspicuous EC and a characteristic tunica media without hyperplasia (Figure 1a). Histological analysis of the aortas from both groups showed normal features, in terms of intimal-to-media ratio and lipid accumulation (data not shown) between the two groups. However, local changes were evident in intimae of the high-cholesterol animals: focal endothelial hyperplasia with some prominent nuclei protruding to the lumen and small clusters of cells evidencing neo-intima rearrangement (Figure 1b).

Upon treatment with a high-cholesterol diet, diffuse hyperplasia was recorded as a higher density of smooth muscle cell (SMC) nuclei in tunica media ( $P < 0.05$ , H-Chol *vs.* C; Figure 1c) with no significant changes in elastic fibres.

In the innermost part of the tunica media, perinuclear halos were observed in high-cholesterol animals compared with the control group (Figure 1b). As these images were negative for Sudan Black staining (data not shown), we speculated that they could be sign of collagen neogenesis. After Masson's trichrome staining, the higher blue intensity in aortas from hypercholesterolaemic animals confirmed this assumption (Figure 1d,e).

#### Effect of diet on arterial remodelling

We analysed the production pattern of PGs in isolated aortic cells, in the setting of hypercholesterolaemia. PGs production was evaluated on microsomal fractions of isolated aortic cells by Western blot.

We detected decorin with a molecular mass of around 100 kDa and its core protein, which migrated faster, with an average size of around 45 kDa (Figure 2a). The quantification of the bands corresponding to the core protein (45 kDa) showed no differences between the two groups (Figure 2b). Nevertheless, we observed that H-Chol group produced around two and a half times less decorin (100 kDa) than the control group ( $P < 0.01$ , H-Chol *vs.* C; Figure 2b). Besides, biglycan expression was poorly detected in aortic cells from the H-Chol group, with a molecular mass of around 100 kDa and a core protein of around 45 kDa ( $P < 0.05$ , H-Chol *vs.* C; Figure 2a,c).

**Figure 1** Histological analyses of aortas. Sections (8–10 μm) from aortas (*n* = 6 per group) from control (a and d) and high-cholesterol-fed rats (b and e) were stained with haematoxylin–eosin (a and b; original magnification 400×) and Masson’s Trichrome (d and e; original magnification 200×). Black arrows point out an area of abundant ECs. SMC hyperplasia at tunica media (c) and focal neo-intimal thickening with higher number of nuclei (black square). Nuclear counting was performed on 20 histological sections per group. \**P* < 0.05.

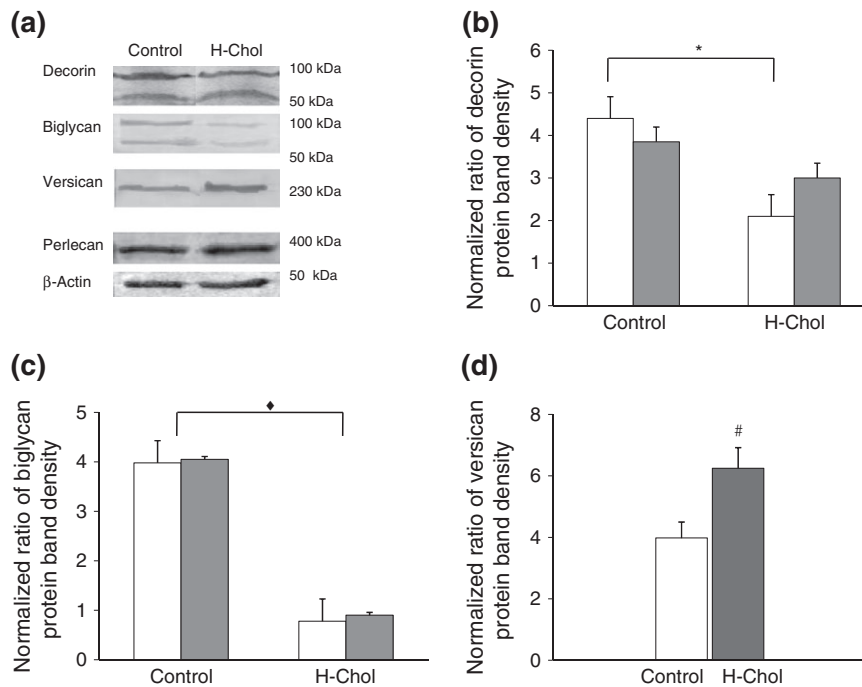
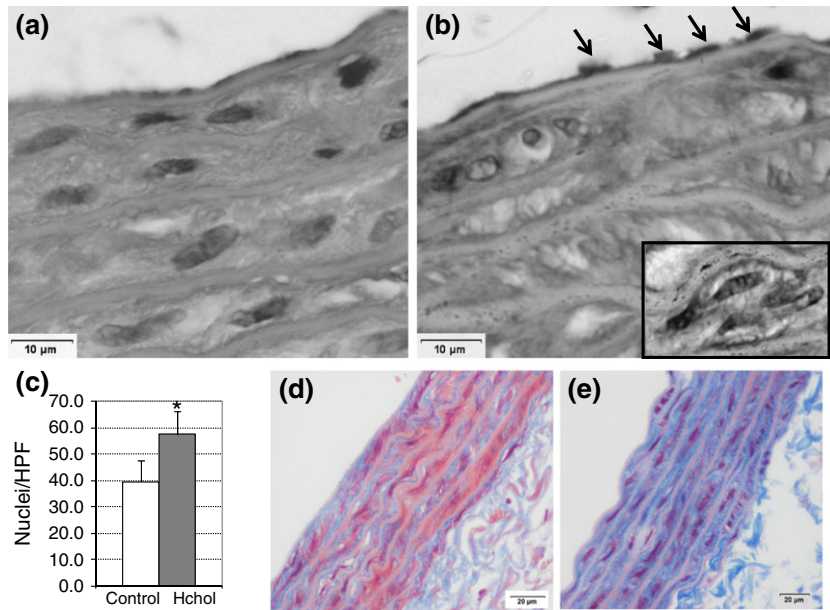


**Figure 2** Particulary proteoglycans (PGs) expression in aortic cells. Aortic ECs and SMCs were isolated and fractionated as described in experimental procedures to obtain microsome fractions. (a) Aliquots of 30 μg of protein were separated by SDS-PAGE and transferred for PG immunological detection. A representative immunoblot for each PG shows (a) decorin (100 kDa) and its core protein (45 kDa); biglycan (100 kDa) and its core protein (45 kDa); versican, after chondroitin ABC digestion and perlecan. β-actin detection was carried out as a loading control (Weng *et al.* 2012). The results are representative of three separate experiments. Densitometric analysis of Western blots. (b) Each column of densitometric analysis represents the relative amount of decorin (100 kDa) – □ – and its core protein (45 kDa) – ■ – in control aortic cells and in the H-Chol group, normalized to protein content. (c) Each column of densitometric analysis represents the relative amount of biglycan (100 kDa) – □ – and its core protein (45 kDa) – ■ – in control aortic cells and in the H-Chol group, normalized to protein content. (d) Each column represents the relative amount of versican in control aortic cells – □ – and in the H-Chol group – ■ –, normalized to protein content. The average of three independent experiments is expressed as mean ± SD (*n* = 3) in each experiment. All microsomal fractions showed similar amount of hydrolysed inorganic phosphate as was compared with reagent blank (10.6 nmol Pi/μg protein *vs.* 0.3 nmol Pi/μg protein, *n* = 3). \*Significant differences in decorin (100 kDa) production between the H-Chol group and the control group (*P* < 0.01). ♦ Significant differences in the production of biglycan (100 kDa) and its core protein (45 kDa) between the H-Chol group and the control group (*P* < 0.05). # Significant differences in versican production between the H-Chol group and the control group (*P* < 0.05).

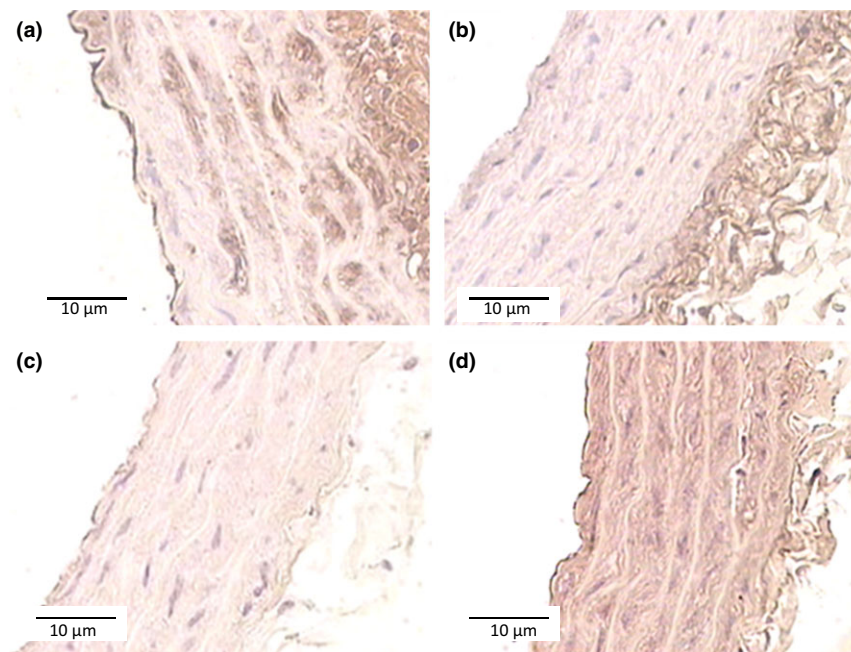


**Figure 3** Immunohistochemistry analyses of aortas. Sections (8–10 µm) from aortas ( $n = 6$  per group), from control (a, and c) and high-cholesterol-fed rats (b and d) were immunostained with anti-decorin (a and b) and anti-versican (c and d) antibodies. Original magnification 200×

**Table 2** Structural characterization of glycosaminoglycans. Densitometric analysis of bands from agarose gel electrophoresis. The results are mean of three different analyses. The coefficient of variation (%) was always found to be lower than 15% for all analyses (Maccari *et al.*, 2011). Number of aortas in each experiment = 3. Chondroitin sulphate (CS), dermatan sulphate (DS) and heparan sulphate (HS)

Treatment groups	CS (%)	DS (%)	HS (%)	CS/DS
Control	15.50 ± 0.07	45.6 ± 0.14	38.9 ± 0.07	0.34 ± 0.02
High cholesterol	23.15 ± 3.04*	38.65 ± 0.78#	38.2 ± 0.02	0.59 ± 0.32♦

\*Significant differences in CS between the H-Chol group and the control group.

#Significant differences in DS between the H-Chol group and the control group.

♦Significant differences in CS/DS between the H-Chol group and the control group.

**Table 3** Structural characterization of glycosaminoglycans (GAGs) by HPLC. The results are mean of three different analyses. The coefficient of variation (%) was always found to be lower than 15% for all analyses (Maccari *et al.*, 2011). Number of aortas in each experiment = 3. ΔDi0s: ΔUA-(1→3)-GalNAc; ΔDi4s: ΔUA-(1→3)-GalNAc-4s; ΔDi6s: ΔUA-(1→3)-GalNAc-6s. The charge density of GAGs obtained from aortas was calculated considering the presence and the percentage of carboxyl and sulphate groups for each disaccharide. 6s/4s: ΔDi6s/ΔDi4s ratio

Treatment groups	ΔDi0s (%)	ΔDi6s (%)	ΔDi4s (%)	Charge density	6s/4s
Control	9.0 ± 0.78	24.2 ± 1.56	66.8 ± 1.98	0.90 ± 0.007	0.36 ± 0.02
High cholesterol	8.75 ± 3.89	27.45 ± 2.76*	63.8 ± 1.31#	0.91 ± 0.04	0.43 ± 0.01♦

\*Significant differences in ΔDi6s between the H-Chol group and the control group.

#Significant differences in ΔDi4s between the H-Chol group and the control group.

♦Significant differences in 6s/4s between the H-Chol group and the control group.

Western blot analysis of isolated aortic cells also detected versican production (Figure 2a). After chondroitin ABC digestion, bands migrating at higher than 230 kDa were observed, with a two-fold increase in versican in the H-Chol group compared with the control ( $P < 0.05$ , H-Chol

*vs.* C; Figure 2d). In addition, perlecan production showed no differences between the two experimental groups (Figure 2a).

Decorin decrease and versican augmentation, compared with the control group, were confirmed by immunohisto-

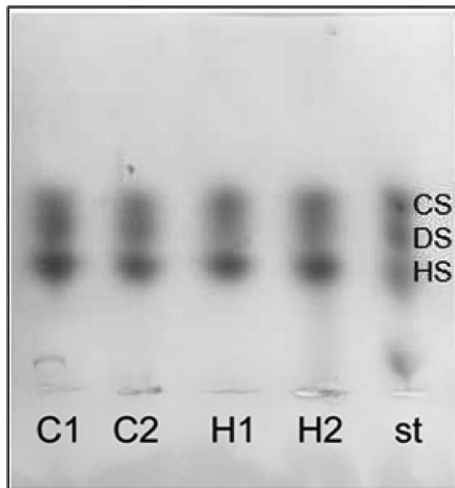


**Figure 4** Agarose gel electrophoresis separation of GAGs (glycosaminoglycan). Glycosaminoglycans were extracted and purified from aortas as described in experimental procedures. Purified GAGs were dissolved in distilled water at a concentration of 1 mg/ml, and 10  $\mu$ l was layered on agarose gel. A representative electrophoresis shows from the top chondroitin sulphate (CS), dermatan sulphate (DS), heparin sulphate (HS) standard; control (C) and hypercholesterolaemic group (H-Chol).

chemistry as shown in Figure 3b,d, respectively. It was not possible to detect biglycan by immunochemistry analyses (data not shown).

#### Structural characterization of Glycosaminoglycans

Glycosaminoglycan chains of PGs have been implicated in divergent functions of the arterial wall, including fibrillar collagen organization, binding to growth factors, low-density lipoproteins (LDL), anti-coagulation and cell migration and proliferation. Therefore, we decided to analyse the chemical characteristics of GAGs of the vascular wall in the setting of

hypercholesterolaemia. Figure 4 illustrates the agarose gel electrophoresis of GAGs extracted from aorta samples of the control and the H-Chol group. No modification of total content of GAGs was found between both experimental groups. In addition, disaccharide characterization was also performed by reverse phase HPLC equipped with fluorescence detector and using differential enzymes: chondroitinase ABC, able to act both on CS and DS, and chondroitinase B, specific only for DS. The results obtained are summarized in Tables 2 and 3. Dermatan sulphate represented the main GAG (45.6%) in aortic cells isolated from control animals, whereas CS showed lower percentage (15.5%). A decreased amount of DS (38.65%) and an increased amount of CS (23.15%) were found in samples obtained from the H-Chol group compared with control. Consequently, the CS/DS ratio was increased in H-Chol group as compared with control animals (Table 2). In contrast, no modification related to heparan sulphate was observed (Table 2).

Hypercholesterolaemic aortic cells showed a significant increase in  $\Delta$ Di6s and a decrease in  $\Delta$ Di4s when compared with control values, with no differences in  $\Delta$ Di0s (Table 3). Thus, the  $\Delta$ Di6s/ $\Delta$ Di4s (6s/4s) ratio was increased in H-Chol group, which reflects a similar increase in the CS/DS ratio, as 6-sulphated disaccharide is generally associated with CS and 4-sulphated disaccharide is related to DS. Finally, no modification of charge density, that is, lower or greater polymer sulphation (Table 3), was found.

#### Analysis of tumour necrosis factor alpha (TNF- $\alpha$ ) mRNA expression in aortas

We decided to analyse the production of TNF- $\alpha$ , the principal cytokine which induces NF- $\kappa$ B activation, in the setting of hypercholesterolaemia.

TNF- $\alpha$  mRNA levels were evaluated in aortic tissues by semiquantitative RT-PCR with TNF- $\alpha$  and  $\beta$ -actin primers. A 1.7-fold increase in TNF- $\alpha$  mRNA was detected in the H-Chol group compared with the control group ( $P < 0.05$ ,

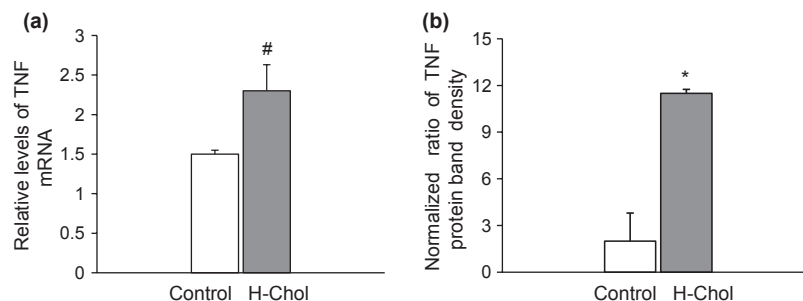


**Figure 5** (a) Analysis of TNF- $\alpha$  mRNA expression by semiquantitative RT-PCR. Aortic tissue was extracted as described in experimental procedures, and RT-PCR was performed with TNF- $\alpha$  and  $\beta$ -actin specific primer pairs. Each column of densitometric analysis represents the relative amount of TNF- $\alpha$  in control –  $\square$  – aortic tissue and in the H-Chol –  $\blacksquare$  – group, normalized to  $\beta$ -actin. Results are expressed as means  $\pm$  SD for duplicate samples from three independent experiments. # $P < 0.05$ . (b) Analysis of TNF- $\alpha$  protein expression in isolated aortic cells by Western blot. Each column of densitometric analysis represents the relative amount of TNF- $\alpha$  in control –  $\square$  – aortic cells and in the H-Chol –  $\blacksquare$  – group, normalized to  $\beta$ -actin protein content. Results are expressed as means  $\pm$  SD for duplicate samples from three independent experiments. \* $P < 0.05$ .

H-Chol *vs.* C; Figure 5a). Besides, TNF- $\alpha$  production was performed by Western blot on the membrane fraction from isolated aortic cells. A significant increase in TNF- $\alpha$  was detected in the H-Chol group ( $P < 0.05$ , H-Chol *vs.* C group; Figure 5b).

These results suggest the presence of a proinflammatory microenvironment within hypercholesterolaemic aortic cells, as revealed by the high levels of TNF- $\alpha$ .

## Discussion

Extracellular matrix remodelling and inflammation are key factors in the development of atherosclerosis. PGs, produced by both endothelial and smooth muscle cells, play a pivotal role in matrix organization and modulation of the activity of growth factors and cytokines. However, the effect of dietary hypercholesterolaemia prior to plaque formation and vascular remodelling is not well established.

In the present study, we used a mammalian hypercholesterolaemic model to detect subtle biochemical and histopathological changes in the intima of aortas. We found that rats fed with a high-cholesterol diet for 30 days developed significant hypercholesterolaemia at expense of non-HDL cholesterol, with no differences either in plasma triglycerides or in HDL cholesterol. Non-HDL-cholesterol increase was primarily due to low-density lipoproteins, intermediate-density lipoproteins and very low density lipoproteins, including highly atherogenic lipoproteins as very low density lipoprotein remnants and to a lesser extent LDL (Joles *et al.* 2000). No differences in plasma triglycerides were observed in our mammalian hypercholesterolaemic model; therefore, the increase in non-HDL cholesterol may be due to LDL rather than triglyceride-rich lipoproteins. Rats are naturally deficient in cholesteryl ester transfer protein (CETP) and therefore relatively resistant to diet-induced atherosclerosis (Hogarth *et al.* 2003; Zak *et al.* 2005). The aortas from the H-Chol group exhibited normal intimal-to-media ratio without lipid accumulation, in agreement with that reported in mammalian models (Joles *et al.* 2000; Deepa & Varalakshmi 2005; Hachani *et al.* 2011). However, hyperplasia of focal endothelial and smooth muscle cells of the intima and evidences of an increase in collagen fibrils density were recorded. In this context, a proinflammatory microenvironment was present as revealed by the high level of TNF- $\alpha$ . Similar results have been previously reported by Hajra and coworkers, who indicated that the NF $\kappa$ B signal transduction pathways in the endothelium of high-probability regions of the pathology were primed to respond to the ingestion of a high-cholesterol diet (1.25%; Hajra *et al.* 2000).

Multiple animal and human studies of the early stage of atherosclerosis have demonstrated a remodelling of the vascular ECM. For instance, biglycan and decorin have been detected in human coronary arteries with diffuse intimal thickening without lipid deposition (Nakashima *et al.* 2007). However, perlecan and biglycan appear in early

lesion with distinct expression patterns as the plaque advances, whereas versican is mostly absent in murine models of atherosclerosis (Kunjathoor *et al.* 2002).

In the present study, Western blots were prepared from the entire aorta, thus representing atherosclerotic and non-atherosclerotic regions considering that only 5–10% of the aorta is affected by plaque development. The results indicate substantial modifications of decorin, biglycan and versican in the aorta in the setting of rat hypercholesterolaemia.

Interestingly, the presence of decorin during fibrillogenesis appears to increase the mechanical properties of collagen gels by preventing the lateral aggregation of fibrils into higher-order structures, which, in turn, may promote longer fibrils that are more interconnected, resulting in a stronger collagen gel (Reese *et al.* 2013).

Together with the results of the present study, attenuation of decorin and biglycan expression might be an effective strategy to inhibit the first step in atherogenesis as detailed in the 'response-to-retention hypothesis' (Tabas *et al.* 2007).

The increase in versican expression observed in aortas from H-Chol animals is noteworthy. Versican could promote the cell proliferation described in Figure 1 either by developing an enriched pericellular environment needed for the proliferative phenotype or by acting as a mitogen itself through the epidermal growth factor sequences in the G3 domain (Evanko *et al.* 1999; Zheng *et al.* 2004).

The structural properties and proportion of PGs are altered during the atherogenic process, in ways that potentially affect their interactions with lipoproteins within the arterial wall. Major structural changes include increases in GAG chain length (Getachew *et al.* 2010) and an increased chondroitin 6-sulphate to chondroitin 4-sulphate ratio (Theocharis *et al.* 2002).

Our analyses of GAG composition revealed a structural modification after feeding rats with a high-cholesterol diet for 30 days, highlighted by an increase in the CS/DS ratio at expense of an increase in CS rather than a decrease in DS. The increased amounts of CS in H-Chol aortas may be due to increased amounts of versican. Although a number of *in vitro* studies indicate that versican is clearly capable of binding to LDL through its CS chains (Cardoso & Mourao 1994), this PG is generally not detected in the lipid-rich centre of the necrotic core, nor does it colocalize with apoE or apoB in mouse atherosclerotic lesions (Kunjathoor *et al.* 2002). Instead, other PGs with DS such as biglycan, or at lower extent decorin, tend to predominate in the lesion. Dermatan sulphate could play protective roles in the arterial wall. It is known that DS chains greatly increase the rate of thrombin inhibition by heparin cofactor II, providing the tissue with anti-atherogenic properties, as thrombin is thought to contribute to atherogenesis, influencing coagulation, chemoattraction and proliferation (Tollefsen 2010; Rasente *et al.* 2012).

In the setting of hypercholesterolaemia, the  $\Delta$ Di6s/ $\Delta$ Di4S ratio was increased in rat aortic cells, which reflects a similar amount in the CS/DS ratio, as CS is mainly composed of 6-sulphated disaccharides, whereas DS is mainly composed of 4-sulphated units. In addition, no modification of charge

density was observed. This last result suggests that no potential GAG elongation or sulphation was induced in aortic cells from rats fed with a high-cholesterol diet. Similar amounts in the CS/DS ratio in human atherosclerotic type II aortas have also been previously reported by Theocharis (Theocharis *et al.* 2002). However, structural characteristics of GAGs chains, elongation and sulfation, which influence lipoprotein binding, seem not to be altered by hypercholesterolaemia (Getachew *et al.* 2010; Anggraeni *et al.* 2011).

Although atherosclerosis occurs within the vessel wall, there is no pharmaceutical treatment that directly targets the blood vessel wall and is capable of preventing the atherosclerotic process (Little *et al.* 2007). Modifying the vessel wall ECM, specifically the PGs component, has been recognized as a primary target for the development of efficacious anti-atherogenic agents. The mechanism by which the CS/DS GAG chains are polymerized *in vivo* is poorly understood. Little and co-worker have described several monosaccharide transferases, which when co-expressed yield GAG polymers (Little *et al.* 2007). Inhibition of these pathways may be a pharmacological therapeutic target to prevent the disease process of atherosclerosis.

In conclusion, we have demonstrated that, in rats, hypercholesterolaemia acts on PGs synthesis and that this could contribute to the prevention of lipid deposition in an inflammatory microenvironment. Our animal experimental model provides further validation of the potential of PGs synthesis as a target for the prevention of atherosclerosis.

## Acknowledgements

Financial support from University of Buenos Aires (20020090200358) is gratefully acknowledged. We thank Rita Yanina Rasente for her critical comments on the manuscript.

## References

- Anggraeni V.Y., Emoto N., Yagi K. *et al.* (2011) Correlation of C4ST-1 and ChGn-2 expression with chondroitin sulfate chain elongation in atherosclerosis. *Biochem. Biophys. Res. Commun.* **406**, 36–41.
- Barfell A., Crumbly A. & Romani A. (2011) Enhanced glucose 6-phosphatase activity in liver of rats exposed to Mg<sup>2+</sup>-deficient diet. *Arch. Biochem. Biophys.* **509**, 157–163.
- Calabrese G.C., Alberto M.F., Tubio R. *et al.* (2004) A small fraction of dermatan sulfate with significantly increased anticoagulant activity was selected by interaction with the first complement protein. *Thromb. Res.* **113**, 43–50.
- Calabrese G.C., Luczak E.N. & Roux M.E. (2009) Importance of CCL25 in the attraction of T cells and the role of IL-7 on the signaling pathways in intestinal epithelial cells. *Immunobiology* **214**, 403–409.
- Camejo E.H., Rosengren B., Camejo G., Sartipy P., Fage G. & Bondjers G. (1995) Interferon gamma binds to extracellular matrix chondroitin- sulfate proteoglycans, thus enhancing its cellular response. *Arterioscler. Thromb. Vasc. Biol.* **15**, 1456–1465.
- Camejo G., Hurt-Camejo E., Wilkund O. & Bondjers G. (1998) Association of lipoproteins with arterial proteoglycans: pathological significance. *Atherosclerosis* **139**, 205–222.
- Cardoso L.E.M. & Mourao P.A.S. (1994) Glycosaminoglycan fractions from human arteries presenting diverse susceptibilities to atherosclerosis have different binding affinities to plasma LDL. *Arterioscler. Thromb.* **14**, 115–124.
- Deepa P.R. & Varalakshmi P. (2005) Atheroprotective effect of exogenous heparin-derivate treatment on aortic disturbances and lipoprotein oxidation in hypercholesterolemic diet fed rats. *Clin. Chim. Acta* **355**, 119–130.
- Evanko S.P., Angello J.C. & Wight T.N. (1999) Formation of hyaluronan and versican-rich pericellular matrix is required for proliferation and migration of vascular smooth muscle cells. *Arterioscler. Thromb. Vasc. Biol.* **19**, 1004–1013.
- Feferman T., Maiti P.K., Berrih-Aknin S. *et al.* (2005) Overexpression of IFN-induced protein 10 and its receptor CXCR3 in myasthenia gravis. *J. Immunol.* **174**, 5324–5331.
- Getachew R., Ballinger M.L., Burch M.L. *et al.* (2010) PDGF  $\beta$ -Receptor kinase activity and ERK1/2 mediate glycosaminoglycan elongation on biglycan and increases binding to LDL. *Endocrinology* **151**, 4356–4367.
- Groeneveld T.W., Oroszlán M., Owens R.T. *et al.* (2005) Interactions of extracellular matrix proteoglycans decorin and biglycan with C1q and collectins. *J. Immunol.* **175**, 4715–4723.
- Hachani R., Dab H., Sakly M. *et al.* (2010) Influence of antagonist sensory and sympathetic nerves on smooth muscle cell differentiation in hypercholesterolemic rat. *Auton. Neurosci.* **155**, 82–90.
- Hachani R., Dab H., Sakly M. *et al.* (2011) The profile of extracellular matrix changes in aorta after sympathectomy in hypercholesterolemic rats. *Auton. Neurosci.* **164**, 67–73.
- Hajra L., Evans A.I., Chen M., Hyduk S.J., Collins Y. & Cybulsky M.I. (2000) The NK-kappa B signal transduction pathway in aortic endothelial cells is primed for activation in regions predisposed to atherosclerotic lesion formation. *Proc. Natl Acad. Sci. USA* **97**, 9052–9057.
- Hogarth C., Roy A. & Ebert D. (2003) Genomic evidence for the absence of a functional cholesteryl ester transfer protein gene in mice and rats. *Comp. Biochem. Physiol. B, Biochem. Mol. Biol.* **135**, 71–81.
- Joles J.A., Kunter U., Janssen U. *et al.* (2000) Early mechanism of renal injury in hypercholesterolemic or hypertriglyceridemic rats. *J. Am. Soc. Nephrol.* **11**, 669–683.
- Kobayashi M., Inoue K., Warabi E., Minami T. & Kodama T. (2005) A simple method of isolating mouse aortic endothelial cells. *J. Atheroscler. Thromb.* **12**, 138–142.
- Kunjathoor V.V., Chiu D.S., O'Brien K.D., & Le Boeuf R.C. (2002) Accumulation of biglycan and perlecan but not versican, in lesions of murine models of atherosclerosis. *Arterioscler. Thromb. Vasc. Biol.* **22**, 462–468.
- Leta G.C., Moura P.A. & Tovar A.M. (2002) Human venous and arterial glycosaminoglycans have similar affinity for plasma low-density lipoproteins. *Biochim. Biophys. Acta* **1586**, 243–253.
- Little P.J., Ballinger M.L. & Osman N. (2007) Vascular wall proteoglycan synthesis and structure as a target for the prevention of atherosclerosis. *Vasc. Health Risk Manag.* **3**, 117–124.
- Maccari F., Buzzega D., Galeotti F. & Volpi N. (2011) Fine structural characterization of chondroitin sulfate in urine of bladder pain syndrome subjects. *Int. Urogynecol. J.* **22**, 1581–1586.
- Nakashima Y., Fujii H., Sumiyoshi S., Wight T. & Sueishi K. (2007) Early human atherosclerosis. Accumulation of proteogly-

- cans and lipids in intimal thickenings followed by macrophage infiltration. *Arterioscler. Thromb. Vasc. Biol.* **27**, 1159–1165.
- Raman K.G., Gandley R.E., Rohland J.D., Zenati M.S. & Tzeng E. (2011) Early hypercholesterolemia contributes to vasomotor dysfunction and injury associated atherogenesis that can be inhibited by nitric oxide. *J. Vasc. Surg.* **53**, 754–763.
- Rasente R.Y., Egitto P. & Calabrese G.C. (2012) Low molecular mass dermatan sulfate modulates endothelial cells proliferation and migration. *Carbohydr. Res.* **356**, 233–237.
- Reese S.P., Underwood C.J. & Weiss J.A. (2013) Effects of decorin proteoglycan on fibrillogenesis, ultrastructure, and mechanics of type I collagen gels. *Matrix Biol.* **32**, 414–423.
- Ross R. (1999) Atherosclerosis is an inflammatory disease. *N. Engl. J. Med.* **340**, 115–126.
- Skalen K., Gustafsson M., Rydberg E.K. et al. (2002) Subendothelial retention of atherogenic lipoproteins in early atherosclerosis. *Nature* **417**, 750–754.
- Tabas I., Williams K.J. & Boré J. (2007) Subendothelial lipoprotein retention as the initiating process in atherosclerosis. Update and therapeutic implications. *Circulation* **116**, 1832–1844.
- Tedgui A. & Mallat Z. (2006) Cytokines in atherosclerosis: pathogenic and regulatory pathways. *Physiol. Rev.* **86**, 515–581.
- Theocharis A.D., Theocharis D.A., De Luca G., Hjerpe A. & Karamanos N.K. (2002) Compositional and structural alterations of chondroitin and dermatan sulfates during the progression of atherosclerosis and aneurysmal dilatation of the human abdominal aorta. *Biochimie* **84**, 667–674.
- Tollefsen D.M. (2010) Vascular dermatan sulfate and heparin cofactor II. *Prog. Mol. Biol. Transl. Sci.* **93**, 351–372.
- Tovar A.M., Cesar D.C., Leta G.C. & Mourao P.A. (1998) Age-related changes in populations of aortic glycosaminoglycans: species with low affinity for plasma low density lipoproteins, and not species with high affinity are preferentially affected. *Arterioscler. Thromb. Vasc. Biol.* **18**, 604–614.
- Volpi N. (2010) High-performance liquid chromatography and on-line mass spectrometry detection for the analysis of chondroitin sulfates/hyaluronan disaccharides derivatized with 2-aminoacridone. *Anal. Biochem.* **397**, 12–23.
- Volpi N. & Maccari F. (2006) Electrophoretic approaches to the analysis of complex polysaccharides. *J. Chromatogr. B Analyt. Technol. Biomed. Life Sci.* **834**, 1–13.
- Weng Z., Greenhau J., Salminen W. & Shi Q. (2012) Mechanism for epigallocatechin gallate induced inhibition of drug metabolizing enzymes in rat liver microsomes. *Toxicol. Lett.* **214**, 328–338.
- Williams K.J. & Tabas I. (1995) The response-to-retention hypothesis of early atherogenesis. *Arterioscler. Thromb. Vasc. Biol.* **15**, 551–561.
- Young G.D. & Murphy-Ullrich J.E. (2004) Molecular interactions that confer latency to transforming growth factor-beta. *J. Biol. Chem.* **279**, 38032–38039.
- Zak Z., Gautier T., Dumont L. et al. (2005) Effect of cholesteryl ester transfer protein (CETP) expression on diet-induced hyperlipidemias in transgenic rats. *Atherosclerosis* **178**, 279–286.
- Zheng P.S., Ven J., Ang L.C. et al. (2004) Versican/PG-M G3 domain promotes tumor growth and angiogenesis. *FASEB J.* **18**, 754–756.
- Zulet M.A., Barber A., Garcin H., Higuere P. & Martínez J.A. (1999) Alterations in carbohydrate and lipid metabolism induced by a diet rich in coconut oil and cholesterol in a rat model. *J. Am. Coll. Nutr.* **18**, 36–42.